J. P. Younger and I. M. Reid
Interferometer angle-of-arrival determination using precalculated phases
Radio Science, 2017; 52(9):1058-1066

DOI: http://dx.doi.org/10.1002/2017RS006284

AGU PUBLICATIONS

Radio Science

RESEARCH ARTICLE
10.1002/2017RS006284

Key Points:
- Angle of arrival can be determined from simultaneous phase differences between all antenna pairs
- Lookup table comparison matches precalculated phases with antenna pair measurements
- Array layouts are not limited and can be three dimensional

Correspondence to:
J. P. Younger,
jyounger@atrad.com.au

Citation:
Younger, J. P., and I. M. Reid (2017), Interferometer angle-of-arrival determination using precalculated phases, *Radio Sci.*, *52*, 1058–1066, doi:10.1002/2017RS006284.

Received 22 FEB 2017
Accepted 2 AUG 2017
Accepted article online 4 AUG 2017
Published online 1 SEP 2017

Interferometer angle-of-arrival determination using precalculated phases

J. P. Younger[1,2] **and I. M. Reid**[1,2]

[1]ATRAD Pty Ltd, Thebarton, South Australia, Australia, [2]School of Physical Sciences, University of Adelaide, Adelaide, South Australia, Australia

Abstract A method has been developed to determine the angle of arrival (AoA) of incident radiation using precomputed lookup tables. The phase difference between two receiving antennas can be used to infer AoA as measured from the pair baseline, but there will be more than one possible solution for antenna spacings greater than or equal to half a wavelength. Larger spacings are preferable to minimize mutual coupling of elements in the receive array and to decrease the relative uncertainty in measured phase difference. We present a solution that uses all unique antenna pairs to determine probabilities for all possible azimuth and zenith values. Prior to analysis, the expected phase differences for all AoAs are calculated for each antenna pair. For a received signal, histograms of possible AoAs for each antenna pair phase difference are extracted and added to produce a two-dimensional probability density array that will maximize at the true value of the AoA. A benefit of this method is that all possible antenna pairs are utilized rather than the restriction to specific pairs along baselines used by some interferometer algorithms. Numerical simulations indicate that performance of the suggested algorithm exceeds that of existing methods, with the benefit of additional flexibility in antenna placement. Meteor radar data have been used to test this method against existing methods, with excellent agreement between the two approaches. This method of AoA determination will allow the construction of low-cost interferometric direction finding arrays with different layouts, including construction of difficult terrain and three-dimensional antenna arrangements.

Plain Language Summary A method has been developed to determine the direction that radio waves are coming from when detected by an arrangement of antennas. The method looks at each of the unique pairs of antennas and compares the received signal with what would be expected for all possible directions. The results from all of the pairs of antennas are added to find the true direction that the radio waves are coming from. This improves the accuracy of simple radars and allows different types of antenna patterns to be used. Computer simulations show that the suggested method is very effective. Tests of data from a real radar also show excellent agreement between the new method and existing techniques.

1. Introduction

Determining the direction of incident radiation is a fundamental function of receive arrays. This work presents an alternative method to determine the angle of arrival (AoA hereafter) that has a high success rate, is computationally efficient, and provides significant flexibility in terms of antenna placement. Meteor radar is used as a test bed and example system, but the methods described can be applied to any array of independent receive antennas for which phase information is available.

One approach to measure the direction of incident radio waves is to use temporal correlation between antennas to track time of flight differences at the antenna locations, but this is costly both in terms of computational burden and the hardware required. Another method is to measure the in-phase and quadrature components of the incident signal on each antenna in a receive array, which provides the phase relative to some reference.

Say two antennas i and j are spaced at a distance d apart and that there is some radiation with wavelength λ incident at an angle ψ to the line connecting the two antennas, as shown in Figure 1. The difference in phase measured between the two antennas will be given by

$$\Phi_{ij} = kd\cos\psi \tag{1}$$

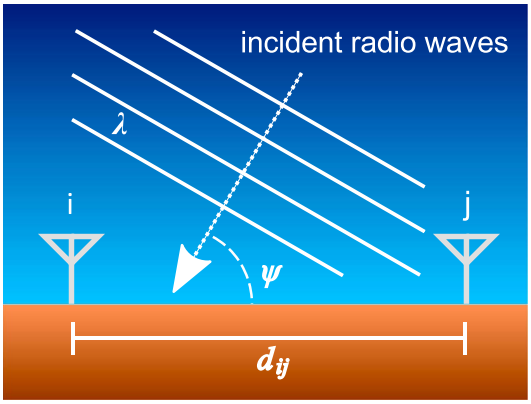

Figure 1. Geometry of radio waves with wavelength λ at an angle-of-arrival ψ relative to the baseline between antennas *i* and *j*, separated a distance d_{ij}.

where $k = 2\pi/\lambda$. Thus, the measured phase difference for an antenna pair can be used to infer the AoA of incident radiation. An additional antenna pair with a component perpendicular to the first pair enables the azimuth and zenith of the received signal to be fully specified.

This relation, however, only provides unambiguous values of ψ when $d < 0.5\lambda$, as the measured value ϕ_{ij} for larger spacings will be aliased into the range $[0, 2\pi]$. Thus, for an antenna pair with separation $n\lambda/2$ there are n possible AoAs that correspond to the measured phase. Without additional information, it is not possible to determine what integer value n is correct in the relation $\Phi_{ij} = \phi_{ij} + n2\pi$. Placing antennas less than 0.5λ apart would seem to be an obvious way of resolving this ambiguity, but closely spaced antennas would suffer from mutual coupling that would distort measured phase as compared to the true phase of the incident wave [*Jones et al.*, 1998; *Younger et al.*, 2013].

Poole [2004] suggested a method to resolve ambiguous AoAs for long baselines with a receive array consisting of three antennas arranged in an isosceles triangle with all $d > 0.5\lambda$ which utilizes a fourth antenna placed outside the triangle at a position chosen to maximize the number of viable AoA estimates. In this configuration the fourth antenna is used to select candidates for the $n2\pi$ term for each antenna pair that produce consistent AoA values.

A more commonly used method for meteor radar receive arrays overcomes the AoA ambiguity of $d > 0.5\lambda$ antenna spacings by constructing each interferometer baseline from two collinear antenna pairs with spacings that differ by 0.5λ, typically 2λ and 2.5λ. The difference between the two collinear pairs provides a $d = 4.5\lambda$ phase difference $\phi_{4.5} = \phi_{2.5} - \phi_{2.0}$ for better angular precision, while the sum of the pairs provides a virtual $d = 0.5\lambda$ phase difference $\phi_{0.5} = \phi_{2.5} + \phi_{2.0}$ for unambiguous AoA determination. While subject to greater relative uncertainty, $\phi_{0.5}$ provides a first estimate of AoA that can be used to infer the factor of 2π to add to value of phase measured across larger antenna spacings [*Jones et al.*, 1998]. A second collinear pair is arranged perpendicular to the first, usually sharing a common antenna, to provide a second value of ψ, enabling azimuth and zenith to be fully determined. *Holdsworth* [2005] improved upon this method by noting that since the difference in phase across antenna pairs is linear with respect to $\sin\psi$, the sine of candidate AoAs should be used to select the best matches in the set of $0.5/2/4.5\lambda$ antenna pairs.

While effective, the $2.0/2.5\lambda$ configuration has several drawbacks. First, the collinear nature of the pairs in each baseline and the specific spacings limits the shape of receive arrays to a cross, L , or T shape with specific lengths. While less of an issue at VHF and smaller frequencies, MF and HF arrays require significant areas to build arrays. It may also be that space is available to construct an interferometric array, but specific locations are not available. An improved method would allow for more flexibility in array layouts.

Second, this method ignores a number of possible antenna pairs by considering each baseline independently. For an array with n antennas, there are $\binom{n}{2}$ unique antenna pairs. This means that for a typical meteor radar receive array with 5 antennas, there are 10 unique antenna pairs, but only 6 are utilized under the method of *Jones et al.* [1998].

Finally, current meteor radar interferometer designs rely on a level antenna array, requiring that antennas and reflector elements be raised to follow variations in the local terrain or arrays to be placed on flat ground. An improved method would allow for vertical variability in antenna position within the array. Arrays with out of plane elements could have the additional benefit of improving zenith estimates near the horizon.

2. Antenna Pair Phase Lookup Tables

A method is proposed to determine direction of radiation incident on a receive array by comparing the difference in phase measured across each antenna pair with tables of precalculated phase differences that would

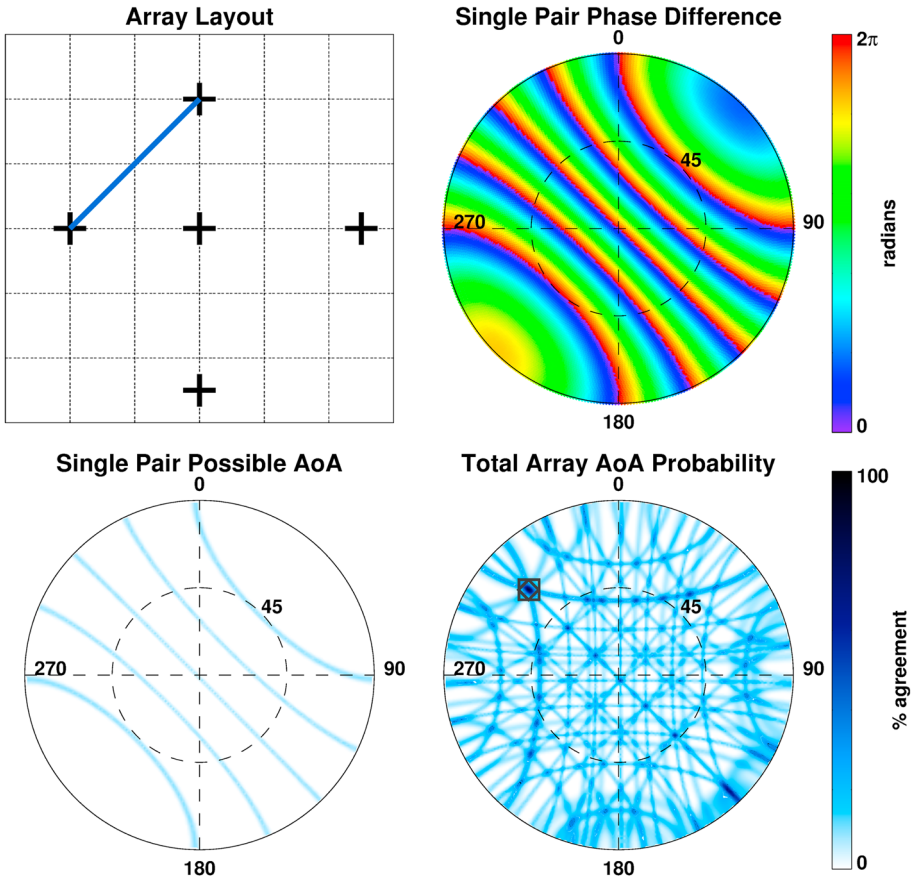

Figure 2. Angle-of-arrival determination using antenna pair lookup tables. (top left) Antenna layout of the Buckland Park meteor radar. Grid lines mark a one wavelength spacing. The blue line highlights the antenna pair considered in Figures 3(top right) and 3(bottom left). (top right) Lookup table of precalculated phases that would be measured for the marked antenna pair for different values of AoA. Azimuth and zenith are mapped to a zenith-centered sky map. (bottom left) Possible AoA values corresponding to the phase difference measured for a single meteor detection recorded 31 January 2016. (bottom right) Image of AoA probabilities assembled from all antenna pairs for a single meteor detection. The diamond shows the AoA selected by the lookup table method, while the square shows the AoA estimated by method described in *Jones et al.* [1998].

be measured for all possible azimuth and zenith values. Let the vector **a** contain the Cartesian components of the AoA vector expressed in terms of azimuth α and zenith β, so that $a_1 = \sin\alpha \sin\beta$, $a_2 = \cos\alpha \sin\beta$, and $a_3 = \cos\beta$. Let the positions of antennas i and j be described by the Cartesian vectors $\mathbf{x}_i$ and $\mathbf{x}_j$, respectively. The phase difference across antenna pair ij is then given by

$$\Phi_{ij} = \frac{2\pi \mathbf{a} \cdot (\mathbf{x}_i - \mathbf{x}_j)}{d_{ij}} \tag{2}$$

Equation (2) can be used to calculate the phase difference for radiation incident at all possible values of azimuth and zenith. The true phase differences Φ_{ij} can then be converted to the observed phase differences ϕ_{ij} that would be measured for a pair of antennas by aliasing the calculated values into the range $[0, 2\pi]$. For all applications described in this work, antenna pair phase differences were calculated on a grid of points spaced approximately uniformly 1° apart across 0–360° azimuth and 0–90° zenith.

Figure 2 shows the precalculated phases for a single antenna pair, with contours of constant phase tracing arcs across the plot of $\phi_{ij}(\alpha, \beta)$. If $d > 0.5\lambda$, there will be more than one contour corresponding to a particular measured phase, due to the aliasing described above.

3. Using Lookup Tables to Determine Angle of Arrival

For a single antenna pair, the contours of constant phase in the lookup table corresponding to the observed phase describe the possible AoAs. Since real systems do not perfectly measure phase, some acceptance

criteria $\Delta\phi$ must be applied to the measured phase. Thus, the set of possible AoAs for a single antenna pair including uncertainty in the phase measurement will satisfy condition

$$\delta\phi = \cos^{-1}\left[\cos\left(\phi_{\text{calc}} - \phi_{ij}\right)\right] < \Delta\phi \tag{3}$$

where ϕ_{calc} is a value of phase for an AoA in the lookup table. This will produce bands of possible AoA values centered on contours of constant phase on the plot of $\phi(\alpha, \beta)$, as shown in Figure 2.

This simple histogram for each antenna pair can be enhanced to produce a better final estimate of AoA. Longer baselines will have a smaller relative error for the same uncertainty in the phase measurement, so a weighting of $d_{ij}(\overline{d})^{-1}$, where $\overline{d}$ is the mean antenna separation, can be applied to each antenna pair's histogram. This was found to have a beneficial effect on the accuracy of compact arrays, where differences in antenna pair separations are small, but arrays with distant outlying elements may experience an increase in false peak detection if this weighting is applied.

An additional weighting can be applied to favor values of the AoA that are closer to the center of the histogram bin, which emphasizes the probability of the AoA being consistent with the measured phase. This was accomplished by assigning a Gaussian weighting with the width of the acceptance band corresponding to 2.5 times the standard deviation, σ. This corresponds to a 99.7% probability of the unbiased phase being within the acceptance band.

Including weighting terms, the AoA probability distribution is given by

$$p(\alpha, \beta) = \begin{cases} \sum \frac{d_{ij}}{\overline{d}} \exp\left[-\frac{\left(\phi_{\text{calc}} - \phi_{ij}\right)^2}{2\sigma^2}\right] & \delta\phi \le \Delta\phi \\ 0 & \delta\phi > \Delta\phi \end{cases} \tag{4}$$

where $\sigma = \frac{2}{5}\Delta\phi$ is the standard deviation of the Gaussian weighting function.

By adding the weighted histograms for all antenna pairs, a probability distribution can be compiled of all values ϕ_{ij} that are within $\Delta\phi$ of the observed phase, as shown in Figure 2. This sum of the histograms of possible AoAs for all antenna pairs is an array of probabilities that provides a measure of the agreement between antenna pair AoA estimates, with a maximum value occurring at the true value of the AoA.

In the case of a meteor radar, physical arguments can be used to restrict the search area for valid values of the AoA. At typical VHF frequencies used, meteor radar detections are improbable below 70 km and above 110 km, so it is only necessary to search for peaks in the probability array of stacked histograms between these heights. The upper and lower height bounds can be converted to upper and lower zenith bounds for each detection from the relation

$$\beta_b = \cos^{-1}\left[\frac{\left(R_\oplus + h_b\right)^2 - R_\oplus^2 - r^2}{(2rR_\oplus)}\right] \tag{5}$$

where $R_\oplus$ is the radius of Earth, h_b is height of the boundary above Earth's surface, and r is the range to the detected meteor from the radar.

If no values in the valid zenith range exceeded the threshold criteria of 0.7, the estimation attempt was deemed to have failed. This particular value was chosen based on modeling, which indicated that it provided a good compromise between sensitivity and false detection rate. Otherwise, the maximum value was labeled as the peak. The initial estimate of the azimuth and zenith was then used to determine the factor of 2π to add to each unique antenna pair's phase difference to de-alias the measured phase. The estimate of AoA can then be precisely determined from a simple weighted average of elements around the peak or by performing a least squares fit of equation (2) using the de-aliased phases of all unique antenna pairs.

Given that the extraction of the original unweighted histograms is a simple Boolean operation and the phases are calculated in advance, this process is quite computationally efficient. Including both weighting terms, a laptop equipped with a 2.4 GHz core-i5 processor was able to process approximately 25 AoAs per second using data from a five-element interferometer.

Table 1. Success Rate and Accuracy of AoA Determination for Numerical Simulations of Different Array Layouts Assuming 5° and 7° Noise in Individual Antenna Phase Measurements

Array Layout	$\sigma = 5°$ Success %	$\sigma = 5°$ Mean Error	$\sigma = 7°$ Success %	$\sigma = 7°$ Mean Error
Cross	99.89	0.67°	99.11	0.90°
Pentagon	99.92	0.58°	99.76	0.79°
Pent. + center	99.99	0.58°	99.59	0.80°
Eq. triangle field	55.56	0.84°	54.16	1.13°

4. Simulated Performance

Two metrics are essential to the validity of an AoA determination algorithm: the ability to successfully determine AoA and the accuracy to which AoA is estimated. The performance of the lookup table-based AoA determination method was evaluated using numerical simulations of a meteor radar like the system at Buckland Park, Australia, described in section 6, as well as a number of other different array configurations.

The field of view of the simulated interferometers was divided into 2113 points uniformly spaced approximately 3° apart across 360° azimuth and 0–85° zenith. For each AoA, the phase of an incident radio wave was calculated for each antenna. Noise was added to each antenna in the form of independent Gaussian error terms with a standard deviation of 7°, corresponding to pair phase difference standard deviation of about 10°, following from *Poole* [2004]. An analysis of Buckland Park meteor radar data indicated that the standard deviation of antenna pair phase differences is approximately 7°, which corresponds to an individual antenna phase measurement noise of about 5°. The simulations were also run with this lower empirically obtained estimate of phase measurement noise for comparison.

The estimated AoA was calculated for every point 100 times with a different seed for the random number generation for uncertainties in each run of the simulation. A phase acceptance width of $\Delta\phi = \pm 30°$ was used to construct individual antenna pair histograms. This value was found in simulations to be sufficiently narrow to avoid excessive false detections. Larger values resulted in lower precision in the estimate of AoA without any improvement in the success rate, while smaller values resulted in a lower rate of successful AoA estimation.

For each test direction, phase differences were calculated for each unique pair in the array, to which a noise error term was added. The sum of noise and the true phase difference was then aliased onto the range $[0, 2\pi]$. The phase differences were then fed into the lookup table algorithm to estimate AoA. If the algorithm returned an estimate within 5°, it was considered successful and the deviation from the original true value of AoA was recorded.

The results of the numerical simulation using different array layouts are listed in Table 1, examples of which are shown in Figure 3. A conventional cross-type interferometer combined a high success rate with an angular precision of less than 1°, although the success rate did decrease with higher antenna noise.

Additional array shapes included an equilateral pentagon with 2.5λ sides, which performed better than the $2.0/2.5\lambda$ cross, both in terms of success rate and angular accuracy. The addition of a central antenna to the pentagonal array resulted in an increase in the rate of successful AoA determination and was also more robust under high noise conditions than the other array designs.

An array of 1.5λ-sided equilateral triangles is an example of an ineffective array, achieving a success rate of only 55.6% with the sky map cut through with wide bands of unresolvable AoAs. This is due to the high level of symmetry in the array and unsufficient diversity of pair separations, which leads to the frequent occurrence of false peaks in the probability density array.

5. Three-Dimensional Arrays

The algorithm's freedom in antenna placement allows flexibility in the construction of interferometric arrays, including three-dimensional interferometers. The collinear pairs used in conventional array layouts discussed in section 1 limit arrays to planar layouts. This can require additional work during array installation if the ground is not level, as well as restricting possible array sites. Three-dimensional arrays can be constructed by

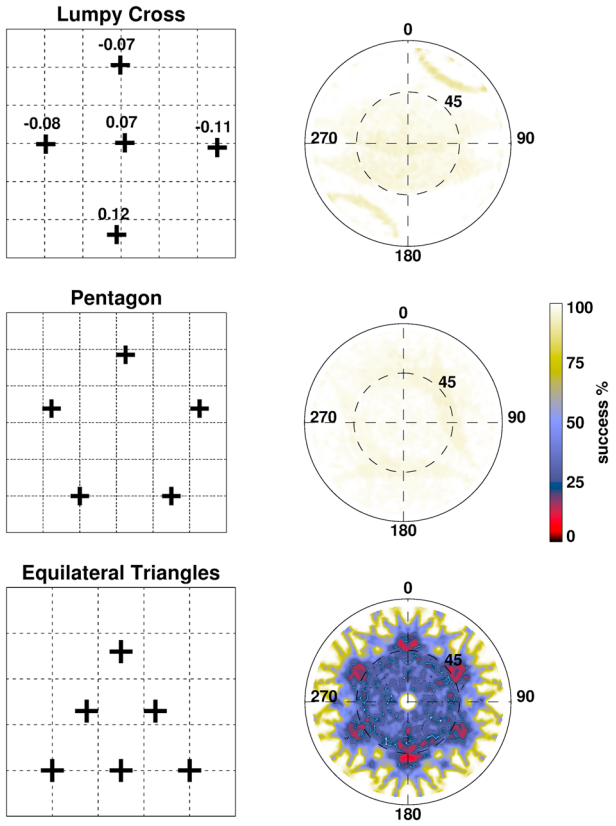

Figure 3. Numerical modeling of AoA determination success rates for different array layouts. (left column) The array layouts, with the numbers above the antenna locations on the lumpy cross showing vertical displacement of each antenna in units of wavelength. Grid lines mark a one wavelength spacing. (right column) A zenith-centered sky map with lighter colors indicating a better success rate of the AoA determination method. Results shown for simulations using individual antenna noise of 7°.

raising or lowering one or more elements out of the plane of the array, which can then be used to infer AoA using the suggested algorithm.

Two three-dimensional arrays are presented for consideration: a lumpy cross and an equilateral pentagon with a raised central element. For the case of a lumpy cross, the standard 2/2.5λ cross was altered with small random displacements to each element, as listed in Table 2. This array represents an attempt to approximate a standard cross array on uneven ground with inexact antenna placement. For the pentagonal array, a central antenna was placed 2.2λ above the plane of a 2.5λ equilateral pentagon, resulting in 3.06λ separations between the raised center and outer antennas.

Numerical simulations summarized in Table 3 show that the lumpy cross yields only slightly degraded performance over the standard cross layout. Similarly, the addition of a raising of the central element of the pentagonal array resulted in only a small reduction in the success rate for AoA determination.

Table 2. Antenna Positions for a Numerically Simulated 2/2.5λ Cross Array With Small Random Displacements to Antenna Positions

Antenna Number	*x* Position	*y* Position	*z* Position
1	0.10	0.02	0.07
2	2.52	−0.11	−0.11
3	−0.11	−2.39	0.12
4	−0.02	2.06	−0.07
5	−1.97	−0.02	−0.08

Table 3. Success Rate, Accuracy, and Zenith Angle Accuracy of AoA Determination for Numerical Simulations of Different Array Layouts Assuming 5° Noise in Individual Antenna Phase Measurements[a]

Array Layout	Success %	Mean Error	Mean Zenith Error
Cross	99.89	0.67°	0.57°
Lumpy cross	99.86	0.67°	0.57°
Pent. + center	99.99	0.58°	0.49°
Pent. + raised center	99.74	0.38°	0.27°

[a]Zenith error was calculated as the average difference between true zenith and estimated zenith over all simulation runs of all AoAs.

The elevation of the central element in the pentagonal array has the benefit of increasing the overall angular precision. Furthermore, the mean absolute error in the zenith angle estimate is almost halved with a raised central element.

The height of a meteor detection at a range R and zenith angle θ with Earth radius R_E is given by

$$h = \sqrt{R_E^2 + R^2 + 2RR_E \cos\theta} - R_E \tag{6}$$

from which it can be seen that errors in zenith estimation can significantly degrade the accuracy of height estimates for meteors detected near the horizon. As most meteor detections occur closer to the horizon, due to the larger sampling volumes at a given height farther away from zenith, a large portion of meteor radar data is limited in height resolution by zenith angle estimate precision. Any improvement to zenith angle accuracy will improve the quality of meteor radar derived winds and vertical diffusion coefficient profiles.

Zenith errors were characterized by the mean zenith component of the AoA error over the 100 simulations with randomized noise at each AoA. Figure 4 clearly shows a significant improvement in near-horizon zenith angle estimates when using a raised central element.

6. Comparison With Meteor Radar Data

Data from a 55 MHz ATRAD meteor radar located at Buckland Park, Australia, was used to compare AoAs estimated from the phase lookup table algorithm with the conventional method described by *Holdsworth* [2005]. Installed in 2006, this system is similar to that described by *Holdsworth et al.* [2008]. Originally, using a valve transmitter at an average power of 7 kW, it was upgraded in 2008 to solid state unit to transmit a peak power of 40 kW on an 8.25% duty cycle [*McIntosh*, 2009]. A single-folded dipole antenna is used for transmission to achieve all-sky coverage. Reception is performed by a five-element interferometer laid out in a cross pattern, with two perpendicular baselines consisting of antennas spaced at 2.0λ and 2.5λ from a central antenna, as shown in Figure 2.

The Buckland Park meteor radar uses the method described by *Jones et al.* [1998] with improvements by *Holdsworth* [2005] to determine the AoA of radio waves scattered by meteors. Each detection record contains, among other information, the estimated AoA and the phases measured between the antenna pairs used. Thus, it is possible to extract the measured phase for each antenna, infer the phase differences on all unique antenna pairs, and directly compare the performance of a conventional $2.0/2.5\lambda$ interferometer AoA finding algorithm with that of a precalculated phase lookup table-based algorithm.

Buckland Park meteor radar data from January 2016 was analyzed using both the conventional method of *Jones et al.* [1998] with the improvements described by *Holdsworth* [2005] and the lookup table method. In total, there were 111,668 detections made across 31 days of operation.

The comparison of a lookup table-based AoA determination method with the $2.0/2.5\lambda$ method yielded a 97.4% agreement rate. The results of the two methods were classed as agreeing if they produced AoA estimates that were separated by less than 5°, with the detections satisfying this condition having a mean angular deviation of 0.33°. With regard to the 2.6% of meteor detections that did not agree to within 5°, a comparison of the results of numerical simulations with the extensive numerical modeling shown in *Holdsworth* [2005] indicates that the lookup table method is the more reliable method of the two in ambiguous cases, based on

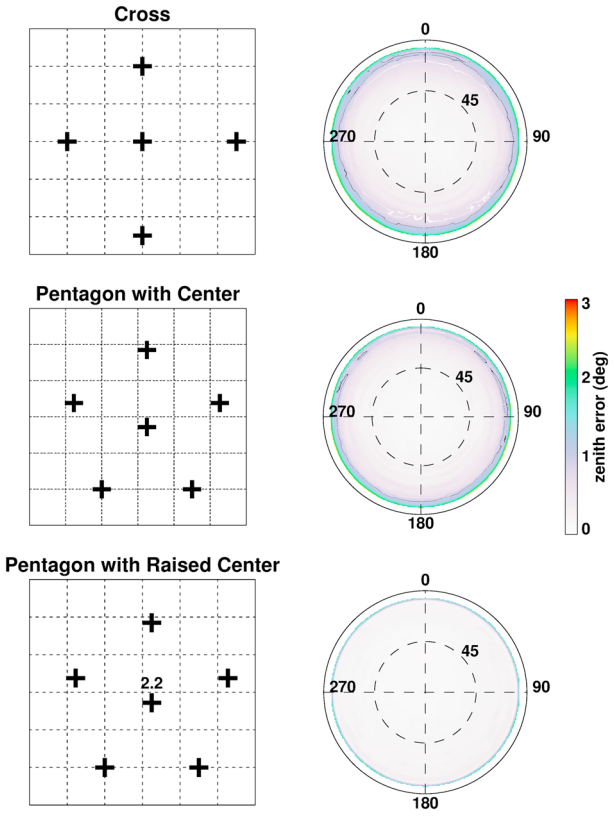

Figure 4. Numerical modeling of zenith angle accuracy for different array layouts. (left column) The array layouts, with the numbers above the antenna locations on the lumpy cross and pentagon with a raised central element showing vertical displacement of each antenna in units of wavelength. Grid lines mark a one wavelength spacing. (right column) A zenith-centered sky map with dark colors indicating larger errors in the zenith angle estimate. Results shown for simulations using individual antenna noise of 5°.

the higher success rate of the lookup table method in simulations. This is likely due to the susceptibility of the Jones method to wraparound, in which phase errors can alias AoA candidates onto the wrong candidate.

7. Summary

The angle of arrival of radio waves incident on an array of independent receive antennas can be determined by comparing the phase differences measured between each unique antenna pair with tables of precalculated phases for all possible AoAs. By adding the histograms of possible AoAs for all antenna pairs, an AoA probability density for the entire array can be used to determine the direction of incident radiation. This method has the immediate advantage of using all unique antenna pairs in an array, as opposed to the restriction to specific pairs used in existing algorithms.

Numerical simulations show that this method performs better than an existing method utilizing the comparison of collinear pairs in specially constructed arrays. This has been confirmed by a direct comparison of algorithms using real-world radar data, which showed excellent agreement between the suggested method and established techniques. This method will allow more flexibility in antenna placement and array design, including constructing of three-dimensional interferometer arrays.

Acknowledgments
This work was completed with the generous financial support of ATRAD Pty Ltd. Data from the Buckland Park meteor radar are available from the University of Adelaide upon request.

References

Holdsworth, D. A. (2005), Angle of arrival estimation for all-sky interferometric meteor radar systems, *Radio Sci.*, *40*, RS6010, doi:10.1029/2005RS003245.

Holdsworth, D. A., D. J. Murphy, I. M. Reid, and R. J. Morris (2008), Antarctic meteor observations using the Davis MST and meteor radars, *Adv. Space Res.*, *42*, 143–154, doi:10.1016/j.asr.2007.02.037.

Jones, J., A. R. Webster, and W. K. Hocking (1998), An improved interferometer design for use with meteor radars, *Radio Sci.*, *33*, 55–66.

McIntosh, D. L. (2009), Comparisons of VHF meteor radar observations in the middle atmosphere with multiple independent remote sensing techniques, PhD thesis, The Univ. of Adelaide, Adelaide, Australia.
Poole, L. M. G. (2004), A simplified interferometer design for use with meteor radars, *Radio Sci.*, *39*, RS2027, doi:10.1029/2002RS002778.
Younger, J. P., I. M. Reid, and R. A. Vincent (2013), Mutual coupling of antennas in a meteor radar interferometer, *Radio Sci.*, *48*, 118–121, doi:10.1002/rds.20026.